# Novel PI-type Direct Power Control Applied on Grid-tied VSIs

Panos C. Papageorgiou, and Antonio T. Alexandridis

***Abstract*— Grid-tied voltage source inverters (VSIs) play the role of a controlled power interface between different power production units and the ac grid. Instead of the usual cascade control scheme of a VSI with current proportional-integral (PI) inner-loops and voltage or even power PI outer-loops, a direct power control (DPC) scheme is considered. DPC is implemented through one stage PI-type controllers that directly regulate the active and reactive power flow. The process does not require a synchronization mechanism, known as phase-locked loop (PLL) but clearly introduces a zero open-loop pole. In the paper, the proposed control scheme realizes PI-type direct active and reactive power regulators, stabilized on the left of the imaginary axis by introducing suitable damping terms. Since this has a clear impact in steady-state error, an appropriate mechanism is proposed which allows the damping term action exclusively during the transient period. Another design innovation introduced by the proposed controller is its robustness against ac voltage variations and system parameters since it does not include the conventionally used decoupling terms. The full nonlinear plant and control scheme is extensively analyzed for its stability and convergence characteristics by applying a rigorous Lyapunov based methodology. Further evaluation of the proposed approach is finally provided by suitable simulations.**

## I. Introduction

Modern power grids are effectively shifting towards a decentralized structure and manner of operation, following the large-scale penetration of mostly geographically dispersed renewable energy sources (RES) [1]. In this process, power converters play a major role in interfacing distributed generation (DG) to the main grid, by offering a wide array of local control capabilities, such as independently regulated active and reactive power transfer and grid-supporting ancillary services. Especially, three-phase voltage source inverters (VSI) currently hold a dominant place among DG configurations in the present grid paradigm, given their direct contribution to the overall system operation [2].

In this frame, significant research effort is now being directed to developing reliable and efficient control schemes in order to establish seamless active and reactive power flow exchange through grid-tied VSIs, regardless of any disturbances introduced by the interfaced DG sources or by the grid itself. Conventional control schemes aiming to achieve this task are mainly based on the well-known Park transformation, which provides dc quantities of three-phase sinusoidal signals in the synchronously rotating reference frame and therefore facilitates the design of appropriate control schemes, such as the ones established upon the vector current control (VCC) notion [3]. In this kind of implementations, typically proportional-integral (PI)-based cascaded schemes are deployed, in which fast inner-loop regulators are driven by slower outer-loop voltage or power controllers. Note, however, that this process requires a synchronization mechanism known as phase-locked loop (PLL) in order to obtain the grid voltage frequency and phase [4].

Hence, in grid-tied VSI configurations featuring VCC-based schemes, a PLL mechanism is standardly employed without much consideration, especially when the grid connection is characterized as a stiff one. Nevertheless, recent studies have suggested that PLL dynamics can have a significant impact on a wider system scale [5]. In particular, the fast action of these control loops can interact with both the grid electromagnetic transients and the electromechanical dynamics of other components in the grid i.e., synchronous generators, potentially leading to instability phenomena [6]. Moreover, the PLL dynamic action has been also identified as a contributing factor in affecting the VSI terminal frequency [7], a fact that gains particular significance when considering the wide VSI-based DG integration in modern power grids. Therefore, more advanced approaches have proposed the deployment of alternative designs for such configurations that do not require PLL mechanisms [8].

An interesting method in this direction is based on the notion of voltage-modulated direct power control (VM-DPC) according to which, both current and voltage quantities are transformed in the stationary $\alpha\beta$-reference frame and subsequently an equivalent active and reactive power dynamic model is obtained. The active and reactive power transfer to the grid is then directly and independently regulated via simple PI-kind compensators, achieving adequate steady-state performance [9]. Although this approach presents several advantages over their counterpart techniques in DPC design, such as passivity-based [10] or model-predictive implementations [11], it still suffers from considerable drawbacks. Specifically, most of the proposed designs are mainly concerned in achieving high degrees of steady-state performance, with minimal consideration for the transient dynamic response of the system. In addition, most studies in this context usually neglect the dc-side dynamics by assuming a constant voltage source applied to the VSI, and thus omitting quite impactful dynamic interactions. Moreover, it is quite often to include feedforward decoupling and other voltage cancellation terms, which are strongly dependent on the system parameters and grid voltage stiffness. Finally, investigations of stability properties in these cases are mostly based on a linearized version of the system, which hold true only around a specific operating point [8].

P. C. Papageorgiou and A. T. Alexandridis are with the Department of Electrical and Computer Engineering, University of Patras, Rion 26504, Greece. Emails: (papageorgiou,a.t.alexandridis)@ece.upatras.gr

Having this in mind, a novel VM-DPC-based control scheme for the case of a grid-tied VSI is presented in this work, that introduces substantial advantages on several aspects. In particular, one of the main aims of the proposed design is to enhance the VSI dynamic behavior by incorporating an innovative integral damping mechanism in its structure, which enables faster and smoother power response. This mechanism is specifically designed so as to act only during transient dynamic periods, i.e. during disturbances, and not to affect the steady-state operation of the VSI. Furthermore, the presented control scheme is based on the complete model of the grid-tied VSI configuration and takes into account the dc-side voltage dynamics as well. Considering this, a novel way of directly providing the duty-ratio input signals to the power inverter is also employed by avoiding a problematic division by the dc voltage state variable. Moreover, this design is entirely independent from system parameters and thus, it serves for another main goal; to establish robustness in variations in system characteristics and to achieve wide applicability to a wide array of such implementations. The resulting closed-loop system comprising the direct power control loops is also rigorously analyzed for its stability and state convergence properties by employing advanced nonlinear analysis tools, while the enhanced and stable behavior of the examined system is verified by conducting through simulation procedures.

## II. Controlled System Description

### A. DPC-based Modeling of Grid-connected VSI

The considered grid-tied VSI layout is presented in the single-line diagram of Fig. 1, wherein the three-phase inverter is connected to an infinite bus through an RL filter. On the dc-side of the VSI, a dc-current source is employed to represent any strongly output regulated DG unit interfaced by the inverter [4].

By adopting the stationary αβ-reference frame, as well as the mean-value model for the action of the VSI switching elements, the open-loop dynamic model that describes the grid-tied configuration is obtained as

$$L\dot{I}_\alpha = -RI_\alpha + u_\alpha V_{dc} - V_\alpha \tag{1}$$

$$L\dot{I}_\beta = -RI_\beta + u_\beta V_{dc} - V_\beta \tag{2}$$

$$C\dot{V}_{dc} = -\left(3/2\right)\left(u_\alpha I_\alpha + u_b I_\beta\right) - \frac{V_{dc}}{R_s} + I_s \tag{3}$$

where the system states $I_\alpha$ and $I_\beta$ represent the α- and β-components of the three-phase grid-side currents $I_{abc}$ in the considered stationary reference frame, while $V_{dc}$ represents the dc-side voltage dynamics of the VSI. The external, uncontrolled inputs of the formulation are provided as $V_\alpha$ ,$V_\beta$ and $I_s$, with the first two inputs expressing the infinite bus voltage magnitude in the stationary αβ-reference frame, while the latter term describes the dc-side current that is being provided by an arbitrary DG source. The controlled inputs of the system, namely the VSI duty-ratio signals, are defined as $u_\alpha = V_{\alpha,inv}/V_{dc}$ and $u_\beta = V_{\beta,inv}/V_{dc}$, respectively, with $V_{\alpha,inv}$ and $V_{\beta,inv}$ being the α- and β-axis voltage components of the three-phase VSI output voltage quantity $V_{abc,inv}$. Finally, on the dc-side of the layout, the considered capacitor features a parallel parasitic resistance, typically of great ohmic value, represented by $R_s$, whereas on the ac-side, the filter resistance and impedance are described by $R$ and $L$.

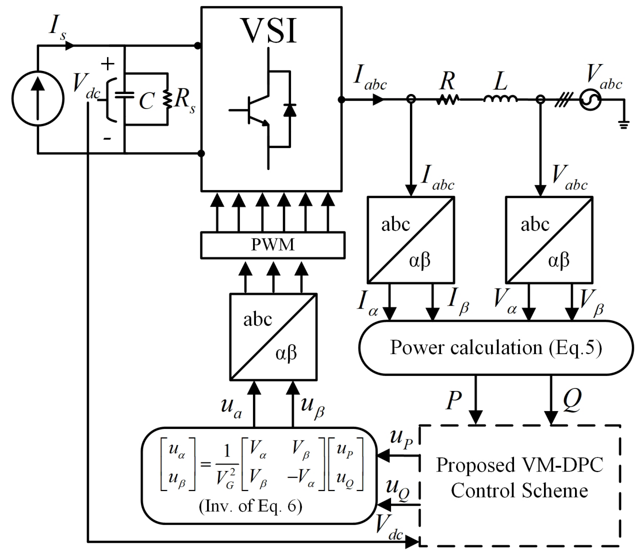


Fig. 1. Scheme of grid-connected VSI.

Since, the three-phase inverter is connected to a stiff grid, the voltage of the infinite bus can be adopted in the same stationary reference frame as [12]:

$$V_\alpha = V_G sin\left(\omega_s t\right),\ \ V_\beta = -V_G cos\left(\omega_s t\right) \tag{4}$$

where $\omega_s$ is defined as the grids' angular frequency, $V_G = \sqrt{V_\alpha^2 + V_\beta^2}$ represents the grid voltage magnitude, and $V_{\alpha\beta}$, represent the corresponding α- and β- components of a symmetric three-phase terminal grid voltage $V_{abc}$. Having defined both voltage and current dynamics in the considered reference frame, the instantaneous fundamental real and reactive power components being provided to the grid by the VSI can then be obtained as well, in the following form:

$$P = (3/2)(V_\alpha I_\alpha + V_\beta I_\beta)\,,\ Q = (3/2)(V_\beta I_\alpha - V_\alpha I_\beta) \tag{5}$$

Considering (1)-(3) and (4) and by differentiating $P$, $Q$ of (5) with respect to time, while also defining the controlled duty-ratio input signals as

$$\begin{bmatrix} u_P \\ u_Q \end{bmatrix} = \begin{bmatrix} V_\alpha & V_\beta \\ V_\beta & -V_\alpha \end{bmatrix} \begin{bmatrix} u_\alpha \\ u_\beta \end{bmatrix} \tag{6}$$

the open-loop system of (1)-(3) can be restated in the following form

$$\left(2/3\right) L\dot{P} = -\left(2/3\right) RP - \left(2/3\right)\omega_s LQ + u_P V_{dc} - V_G^2 \tag{7}$$

$$\left(2/3\right) L\dot{Q} = \left(2/3\right)\omega_s LP - \left(2/3\right) RQ + u_Q V_{dc} \tag{8}$$

$$V_G^2 C\dot{V}_{dc} = -u_P P - u_Q Q - V_G^2 V_{dc}/R_s + V_G^2 I_s \tag{9}$$

In this formulation the duty-ratio signals $u_P$ and $u_Q$ are equivalent to the ones obtained by adopting the well-known synchronously $dq$-rotating frame approach, i.e. $u_P$=$u_d$ and $u_Q$=$u_q$. Noteworthy, a PLL mechanism is not required for this transformation, however, in order to obtain the resulting three-phase modulation signals, an inverse transformation has to be performed, by first obtaining the αβ-reference frame quantities and then transforming them back into the *abc*-reference frame system, as displayed in Fig. 1.

### B. DPC-based Design with Dynamic Integral Damping

Generic grid-tied control schemes based on the VM-DPC principle have been proven to benefit from the absence of PLL mechanisms [8], by avoiding adverse dynamic interactions and therefore by displaying enhanced performance compared to other VCC-based implementations. Nevertheless, the conventional procedure of designing such formulations involves the employment of feed-forward decoupling and other cancellation terms, as displayed in Fig. 2.

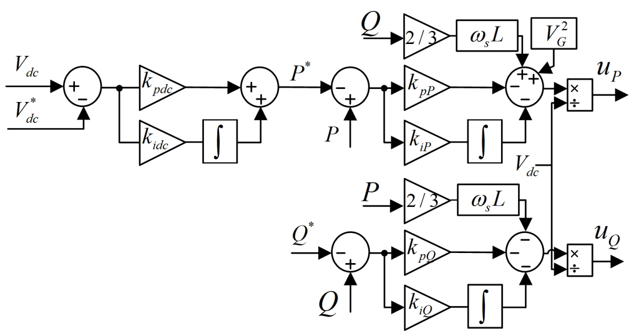

Fig. 2. Conventional DPC block diagram.

Although, this approach leads to a simpler and easier to handle closed-loop system, it also creates a strong dependence of the controllers from systems parameters. In addition, when the dc-side dynamics are also included in the model formulation, the controlled duty-ratio input signals have to be divided by a state variable, namely the $V_{dc}$, and thus several implications emerge regarding possible instability phenomena in transient conditions, as well as higher harmonic in the controlled states.

Thus, in order to independently and efficiently control the VSI output active and reactive power, a novel model-based control scheme has been developed, which effectively withdraws all of the aforementioned drawbacks. In particular, the proposed design comprises a pair of PI-type power regulators, incorporating also an additional damping-like term in their formulation as

$$u_P = -k_{pP}\left(P - P^*\right) - k_{iP}Z_P \tag{10}$$

where

$$\dot{Z}_P = P - P^* - \bar{k}_{if}\left(\xi_P\right)Z_P \tag{11}$$

and the corresponding regulator for the reactive power flowing to the grid as

$$u_Q = -k_{pQ}\left(Q - Q^*\right) - k_{iQ}Z_Q \tag{12}$$

with

$$\dot{Z}_Q = Q - Q^* - \bar{k}_{ig}\left(\xi_Q\right)Z_Q \tag{13}$$

It can be easily observed that (11) and (13) represent the integral terms of the active and reactive power PI controllers of (10) and (12). In general, the inclusion of extra damping-like terms, as those introduced in (11) and (13), in the integral part of the regulator is expected to enhance the dynamic behavior of the controlled system. As it has been established by similar leaky-integrator PI-based implementations [12], this is achieved by increasing its dissipative characteristics.

Our intention is to insert a variable gain in both (11) and (13), which however should converge to zero as $t \to \infty$. An obvious choice would be to define the terms $\bar{k}_{if}\left(\xi_P\right)$ and $\bar{k}_{ig}\left(\xi_Q\right)$ as a function of the deviation between active power and reactive power, with their references, i.e. $(P - P^*)$ and $(Q - Q^*)$, which correspond to $\dot{Z}_P$ and $\dot{Z}_Q$, respectively. In this case, both these damping-like terms should zero-out over time, establishing a vanishing dissipation, however it is not guaranteed that they would keep at all times a positive value; in fact if these terms obtain a negative value at some point during a transient period, they would actually reduce the damping properties of the system. To this end, we simply define $\bar{k}_{ir}\left(\xi_s\right) = k_{ir}\dot{Z}_s^2$, where $r = f, g$ and $s = P, Q$, aiming to preserve a non-negative, and of higher impact dissipation through these terms.

Another interesting aspect of the proposed control design is that it does not incorporate any decoupling terms, as it is typically done with implementations represented by Fig. 2. In this manner the proposed regulators have no dependence from the system parameters, as it can be clearly observed in the control block diagram of Fig. 3. As an immediate result, this scheme offers extended applicability to a wide array of grid-tied VSI configurations, by not being affected by filter parameter variations or grid voltage disturbances. Furthermore, the duty-ratio signals are directly provided to the VSI and thus, the potentially problematic division by the dc-link voltage, namely $V_{dc}$, is avoided. Of course, the benefit of the latter novelty extends also to the quality of the controlled inputs, which feature less harmonic distortion.

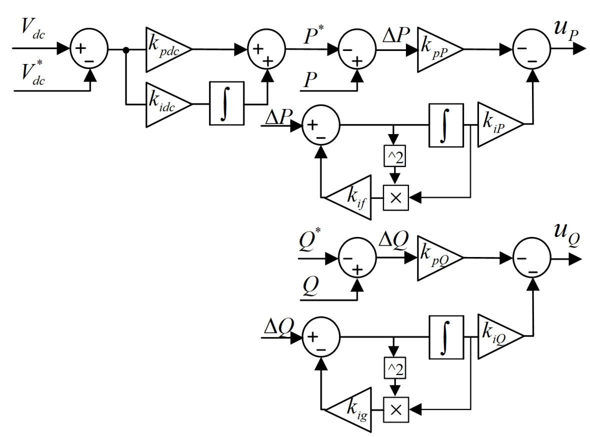

Fig. 3. Proposed control block diagram.

Since the complete VSI model is considered in the scope of this work, the dc-link voltage dynamics play a key role to the overall performance of the system as well. In particular, the reference of the active power fed to the grid by the VSI is determined by the product of the $V_{dc}$ voltage magnitude and the dc current being provided by the interfaced RES, which is considered strongly regulated in this case. Hence, it is typically desired to control the dc-side voltage to a specific value, as a means to regulate the actual active power injection to the grid. This is achieved by introducing an outer-loop voltage controller of simple PI-type as

$$P^* = k_{pdc}\left(V_{dc} - V_{dc}^*\right) + k_{idc}\int\left(V_{dc} - V_{dc}^*\right)d\tau \qquad (14)$$

with $V_{dc}^*$ being a desired positive dc-voltage reference value.

## III. Stability Analysis

Having in mind the structure of the regulators introduced in (10) and (12), it is crucial to establish strong stability conditions for the controlled VSI system. This is mainly because the actual dynamic integral damping introduced via (11) and (13) is only accomplished through the convergence of all system states to equilibrium. In this frame, a detailed nonlinear stability analysis is considered, that guarantees this dynamic action is only limited through transients periods and does not cause any offset in power regulation.

In order to proceed with the stability evaluation of the closed-loop system, and by also considering the time-separation principle applied in cascaded control loops [3], the faster and of high dynamic impact inner-loop active and reactive power controllers of (10)-(13) are incorporated into the VSI plant of (7)-(9):

$$\frac{2}{3}L\dot{P} = -\frac{2}{3}RP - \frac{2}{3}\omega_s LQ + u_P\widetilde{V}_{dc} - \bar{k}_{pP}(P - P^*) - \bar{k}_{iP}Z_P - V_G^2 \qquad (15)$$

$$\frac{2}{3}L\dot{Q} = \frac{2}{3}\omega_s LP - \frac{2}{3}RQ + u_Q\widetilde{V}_{dc} - \bar{k}_{pQ}\left(Q - Q^*\right) - \bar{k}_{iQ}Z_Q \qquad (16)$$

$$V_G^2 C\dot{\widetilde{V}}_{dc} = -u_P P - u_Q Q - V_G^2\widetilde{V}_{dc}/R_s + V_G^2\left(I_s - c/R_s\right) \qquad (17)$$

$$\bar{k}_{iP}\dot{Z}_P = \bar{k}_{iP}\left(P - P^*\right) - \bar{k}_{iP}k_{if}\dot{Z}_P^2 Z_P \qquad (18)$$

$$\bar{k}_{iQ}\dot{Z}_Q = \bar{k}_{iQ}\left(Q - Q^*\right) - \bar{k}_{iQ}k_{ig}\dot{Z}_Q^2 Z_Q \qquad (19)$$

with the state vector being $x^T = \left[P\; Q\; \widetilde{V}_{dc}\; Z_P\; Z_Q\right]$, where it is defined: $\widetilde{V}_{dc} = V_{dc} - c$ , with scalar $c > 0$ adopted as in [4]. In this formulation, the following gains are considered positive ones and are provided as: $\bar{k}_{de} = k_{de}c$, for $d = p, i$ and $e = P, Q$ .

Considering the strongly nonlinear structure of the closed-loop system of (15)-(19), the conducted analysis adopts a highly effective framework based on the input-to-state stability (ISS) notion [13], which is capable of handling the investigation of such systems to its full extend. To this end, consider the autonomous system formulation

$$\dot{x} = f\left(x\left(t\right), u\left(t\right)\right) \qquad (20)$$

where $f : \mathbb{R}^n \times \mathbb{R}^m \to \mathbb{R}^n$ is piecewise continuous in $t$ and locally Lipschitz in $x$ and $u$, with the input $u(t)$ being a piecewise constant, continuous, bounded function of $t$ for all $t \geq 0$. Also, consider the unforced version of the system (20), where any external input through vector $u$ is diminished:

$$\dot{x} = f\left(x, 0\right) \qquad (21)$$

At this point the following results are recalled [14], stating the sufficient conditions for a system of the previous form to feature the ISS property:

**Lemma 1.** *Suppose system* (20) *is continuously differentiable and globally Lipschitz in $x$ and $u$, uniformly in $t$. If the unforced system of* (21) *has a globally exponentially stable equilibrium point at the origin, then the system $\dot{x} = f\left(x, 0\right)$ is ISS.*

Having in mind this, a straightforward manner of establishing the ISS property of the complete closed-loop system is to investigate and determine that the origin of (20) is exponentially stable. In order to derive to this conclusion, the following Theorem is also recalled from [14]

**Theorem 1.** *Let $x = 0$ be an equilibrium point of* (21) *and there exist a continuously differentiable function V and non-decreasing functions $\delta_i \in K_\infty$, $\delta_i : \mathbb{R}_{\geq 0} \to \mathbb{R}_{\geq 0}$, for $i = 1, 2, 3$, such that for all $(t, x) \in \mathbb{R}_{\geq 0} \times \mathbb{R}^n$, $\delta_1\left(\|x\|\right)^\nu \leq V\left(t, x\right) \leq \delta_2\left(\|x\|\right)^\nu$ , with time derivative $\dot{V}\left(t, x\right) \leq -\delta_3\left(\|x\|\right)^\nu$, then the origin $x = 0$ is globally exponentially stable (GES).*

Now, consider the following positive definite Lyapunov function for the closed-loop system of (15)-(19)

$$H = \frac{1}{2}x^T Mx. \qquad (22)$$

where $M = diag\left\{\frac{2}{3}L, \frac{2}{3}L, V_G^2 C, \bar{k}_{iP}, \bar{k}_{iQ}\right\}$ .

The time derivative of (22) can then be derived as

$$\dot{H} = -x^T Dx + x^T u. \qquad (23)$$

with matrix $D$ being a positive semi-definite matrix in this case, provided by

$$D = diag\left\{\left(R + \bar{k}_{pP}\right), \left(R + \bar{k}_{pQ}\right), \left(V_G^2/R_s\right) \bar{k}_{iP}k_{if}\dot{Z}_P^2, \bar{k}_{iQ}k_{ig}\dot{Z}_Q^2\right\}$$

and the external input vector is considered as

$$u^T = \left[\left(\bar{k}_{pP}P^* - V_G^2\right)\; \bar{k}_{pQ}Q^*\; V_G^2\left(I_s - c/R_s\right) - \bar{k}_{iP}P^* - \bar{k}_{iQ}Q^*\right].$$

Note that the structure of $D$ is not the typical one, in the sense that the last two diagonal terms are expected to reach zero value in steady-state and therefore, the damping matrix $D$ cannot be strictly defined as a positive definite one, as implied by the conditions of Theorem 1. Nevertheless, these terms also remain nonzero and positive very close to the origin, meaning that the results of Theorem 1 can be adopted as long as $\dot{Z}_P \neq 0$ and $\dot{Z}_Q \neq 0$ (covering the whole $\mathbb{R}^5$ domain, up to a infinitely small region close to the origin). Hence, in order to fully investigate the stability properties of the controlled system, two cases are considered, namely the first one being with $\dot{Z}_P \neq 0$, $\dot{Z}_Q \neq 0$ and secondly, by assuming $\dot{Z}_P = \dot{Z}_Q = 0$.

To proceed with the analysis, the autonomous version (15)-(19) is obtained by setting the external input vector to zero, i.e. $u = 0$, which implies $P^* = Q^* = V_G^2 = 0$ and $I_s = c/R_s$. Then, by taking into account the first case (positive definite matrix $D$), the selected Lyapunov function $H$ satisfies the following conditions

$$\rho_1\left\|x\right\|^2 \leq H \leq \rho_2\left\|x\right\|^2 \qquad (24)$$

with $\rho_1 = min\left\{\frac{1}{3}L_f, \frac{1}{2}V_G^2 C, \frac{1}{2}\bar{k}_{iP}, \frac{1}{2}\bar{k}_{iQ}\right\}$
$\rho_2 = max\left\{\frac{1}{3}L_f, \frac{1}{2}V_G^2 C, \frac{1}{2}\bar{k}_{iP}, \frac{1}{2}\bar{k}_{iQ}\right\}$
and

$$\dot{H} \leq -\rho_3 \left\|x\right\|^2 \tag{25}$$

with $\rho_3 = min\left\{\left(R + \bar{k}_{pP}\right), \left(R + \bar{k}_{pQ}\right), \left(V_G^2/R_s\right)\right\| \bar{k}_{iP} k_{if} \dot{Z}_P^2, \bar{k}_{iQ} k_{ig} \dot{Z}_Q^2 \right\}$.

It is clearly observed, that (24) and (25) indicate that for $\nu = 2$ and for almost all $x \in \mathbb{R}^5$, all the conditions of Theorem 1 are met, and since the (practical) origin of the unforced system is GES, then the ISS property can be established through Lemma 1 for the complete, forced closed-loop system. This property can be further utilized to derive useful results regarding the convergence of system states to nonzero equilibria, as it was recently proven, by considering Theorem 6 from [15]. This practically means that all states would eventually reach a nonzero equilibrium over time and consequently, it would hold that $\dot{Z}_P = \dot{Z}_Q = 0$.

In this case, the structure of matrix $D$ no longer contains the last two integral damping terms and the stability close to the actual origin can be investigated through the local-ISS (l-ISS) notion. Specifically, by considering Lemma 1 and Theorem 1 as presented in [16], it is possible to conclude asymptotic stability inside this infinitely small region containing the origin, through LaSalle's (local) invariance principle and then establish the l-ISS property. Moreover, by also recalling Theorem 2 in [16], state convergence is also guaranteed. Therefore, by taking into account all possible cases, it is concluded that under the assumption of bounded and piecewise constant external input action, all system states converge exponentially to a set in $\mathbb{R}^5$, but when they reach that equilibrium they hold asymptotic stability properties in the l-ISS sense. On the other hand, every disturbance that leads to another nonzero equilibrium would trigger $\dot{Z}_P \neq 0$ and $\dot{Z}_Q \neq 0$ and then the system states would approach globally and exponentially to a different set.

## IV. Simulation Results

In order to investigate the enhanced dynamic behavior that the proposed control design enables and to also validate the stable behavior of the closed-loop system, a thorough simulation procedure was conducted. In particular, the complete controlled grid-tied VSI layout of Fig. 1 was modeled in Matlab/Simulink environment and several scenarios were considered. The results derived from the proposed control implementation were also compared to the ones obtained from simulating a typical DPC-based configuration, under the same conditions. The system parameters were selected as $R = 0.9\,\Omega$, $L = 3.3\,mH$, $C = 10\,mF$, $R_s = 40\,k\Omega$, $V_G = 325\,V$ (peak value), $\omega_s = 100\pi\,r/s$ and the switching frequency for the VSI was set as $f_{sw} = 20\,kHz$. For the regulators, the following gains were considered: $\bar{k}_{pP} = \bar{k}_{pQ} = 1.8$ and $\bar{k}_{iP} = \bar{k}_{iQ} = 70$, whereas the damping term gains were set as $k_{If} = k_{Ig} = 4 \cdot 10^{-6}$. Finally, the outer-loop dc-voltage controller gains as: $k_{pdc} = 300$ and $k_{idc} = 20 \cdot 10^3$, whereas the dc-side voltage reference input was set at $V_{dc}^* = 1200$V.

The first simulation scenario aims to investigate the controlled system behavior under several abrupt external input changes in the dc-side current, $I_s$. Specifically, at time $t_1 = 0.2$s the uncontrolled input of $I_s$ takes the value of 4A from its initial value of 2A, and at time $t_2 = 0.6$s it reduced to 1.8A, whereas at time $t_3 = 0.9$s a change in the reactive power reference is enforced, from $Q^* = 0$ that is set initially, to $Q^* = 1000$Var.

The results presented in Fig. 4-6 reveal a quite satisfactory and overall enhanced performance provided by the proposed VM-DPC scheme. In particular, in Fig. 4, the active power response of the VSI displays significantly lower overshoots compared to the conventional DPC design, while it reaches the corresponding equilibria faster than when the standard method is implemented. The same holds true for the reactive power response of Fig. 5, where it is also verified that the proposed control design presents lower harmonic distortion due to the direct provision of duty-ratio signals. Moreover, a notable difference is observed in the dc-side voltage dynamics as well. Considering Fig. 6, the proposed regulators have a distinctly beneficial impact on the regulation of the dc-voltage, enhancing its dynamic profile in a remarkable manner.

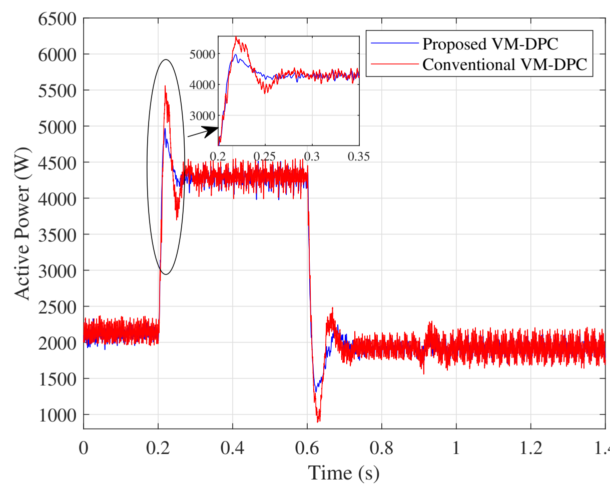


Fig. 4. Response of active power provided to the grid.

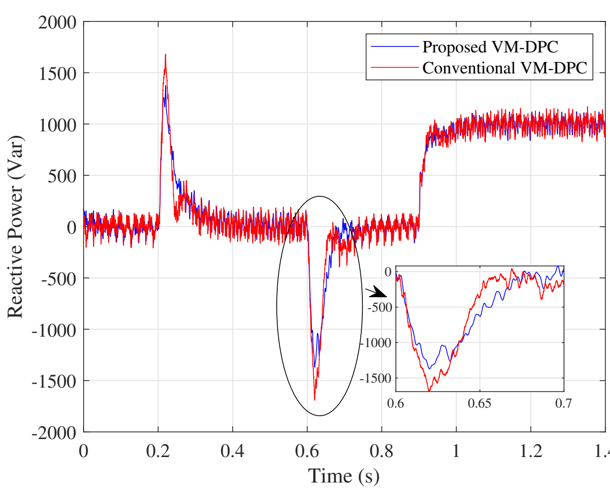


Fig. 5. Response of VSI reactive power output.

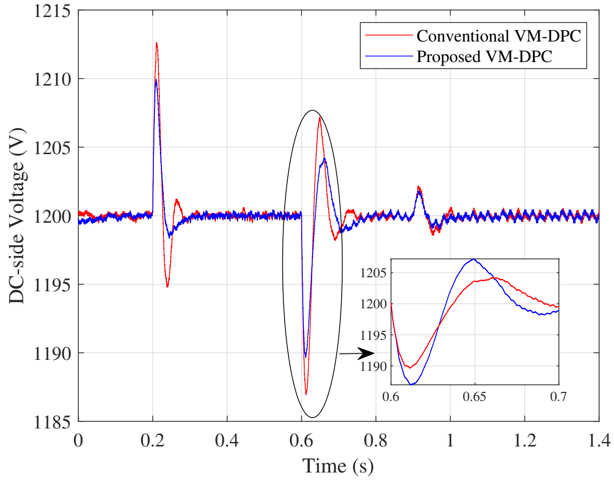


Fig. 6. Dc-side voltage dynamics response.

However, another significant advantage introduce by the novel integral damping control structure is that it is effectively independent of system parameters. In order to better demonstrate this quality, the second scenario examines the control system behavior under a variation of 15% in the filter inductance, i.e. $L = 3.8mH$ and also a sudden grid disturbance. Specifically, the same dc-side input current changes occur in this scenario as well, however at time $t_3 = 0.9$s a grid voltage magnitude reduction of 20% is applied. The superior performance of the proposed control scheme is verified once again by observing the active power response of Fig. 7, particularly during the dc-side current disturbances. Nevertheless, the most impressive result is that it retains the stable closed-loop system behavior even during the major reduction in grid voltage. On the other hand, the system parameter dependent implementations are susceptible to this kind of disturbances and thus, they cannot guarantee stable performance over a wide operating range or under large disturbances.

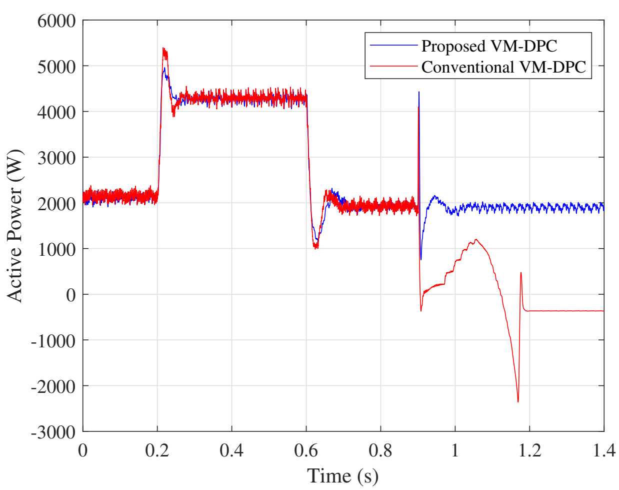


Fig. 7. Active power flow.

## V. Conclusions

A novel VM-DPC design for grid-connected VSI configurations is proposed in this work, which offers several advantages compared to the standard PLL-less DPC schemes. The proposed implementation introduces an integral damping mechanism that significantly enhances the VSI performance during disturbances, while a rigorous nonlinear analysis is also employed to guarantee its stable operation over a large operating range. Since, this design is also completely independent from the system parameters and provides directly the duty-ratio input signals to the power inverter, it is also suitable for applications where parameter variations or external uncontrolled input large disturbances are of concern.

## References


[1] D. Lew, D. Bartlett, A. Groom, P. Jorgensen, J. O Sullivan, R. Quint, B. Rew, B. Rockwell, S. Sharma, and D. Stenclik, “Secrets of successful integration: Operating experience with high levels of variable, inverter-based generation,” *IEEE Power and Energy Magazine*, vol. 17, no. 6, pp. 24–34, 2019.

[2] P. C. Papageorgiou and A. T. Alexandridis, “Controlled impedance-admittance-torque nonlinear modeling and analysis of modern power systems,” *Energies*, vol. 13, no. 10, 2020.

[3] A. Yazdani and R. Iravani, *Voltage-Sourced Converters in Power Systems*. Hoboken, NJ: IEEE/Wiley, 2010.

[4] P. C. Papageorgiou, K. F. Krommydas, and A. T. Alexandridis, “Validation of novel pll-driven pi control schemes on supporting vsis in weak ac-connections,” *Energies*, vol. 13, no. 6, 2020.

[5] Z. A. Alexakis, A. T. Alexandridis, P. C. Papageorgiou, and G. C. Konstantopoulos, “Design of a bandwidth limiting pll for grid-tied inverters with guaranteed stability,” *IEEE Transactions on Sustainable Energy*, vol. 16, no. 2, pp. 774–784, 2025.

[6] N. Hatziargyriou *et al.*, “Definition and classification of power system stability: Revisited extended,” *IEEE Trans. on Power Systems*, vol. 36, no. 4, pp. 3271–3281, 2021.

[7] Y. Wang, X. Chen, Y. Wang, and C. Gong, “Analysis of frequency characteristics of phase-locked loops and effects on stability of three-phase grid-connected inverter,” *International Journal of Electrical Power Energy Systems*, vol. 113, pp. 652–663, 2019.

[8] Y. Gui, C. Kim, C. C. Chung, J. M. Guerrero, Y. Guan, and J. C. Vasquez, “Improved direct power control for grid-connected voltage source converters,” *IEEE Transactions on Industrial Electronics*, vol. 65, no. 10, pp. 8041–8051, 2018.

[9] Z. Gong, C. Liu, Y. Gui, F. F. da Silva, and C. L. Bak, “Power decoupling method for voltage source inverters using grid voltage modulated direct power control in unbalanced system,” *IEEE Transactions on Power Electronics*, vol. 38, no. 3, pp. 3084–3099, 2023.

[10] Y. Gui, G. Lee, C. Kim, and C. Chung, “Direct power control of grid connected voltage source inverters using port-controlled hamiltonian system,” *International Journal of Control, Automation and Systems*, vol. 15, no. 5, pp. 2053–2062, Oct. 2017.

[11] S. Vazquez, J. Rodriguez, M. Rivera, L. G. Franquelo, and M. Norambuena, “Model predictive control for power converters and drives: Advances and trends,” *IEEE Transactions on Industrial Electronics*, vol. 64, no. 2, pp. 935–947, 2017.

[12] P. C. Papageorgiou and A. T. Alexandridis, “A novel pll-less direct power control of vscs,” in *2023 IEEE PES Innovative Smart Grid Technologies Europe (ISGT EUROPE)*, 2023, pp. 1–5.

[13] E. D. Sontag and Y. Wang, “On characterizations of the input-to-state stability property,” *Systems Control Letters*, vol. 24, no. 5, pp. 351–359, 1995.

[14] H. K. Khalil, *Nonlinear Systems*, 2nd ed. Prentice Hall, 2001.

[15] A. T. Alexandridis, “Studying state convergence of input-to-state stable systems with applications to power system analysis,” *Energies*, vol. 13, no. 1, 2020.

[16] P. C. Papageorgiou, A. T. Alexandridis, and G. C. Konstantopoulos, “Improving the dynamic response of pi voltage modulated-direct power controlled grid-tied vsis,” in *2025 European Control Conference (ECC)*, 2025, pp. 1–6.